Building and Environment 156 (2019) 21–32

Contents lists available at ScienceDirect

Building and Environment

journal homepage: www.elsevier.com/locate/buildenv

Inter-/intra-zonal seasonal variability of the surface urban heat island based on local climate zones in three central European cities

Jan Geletič[a,b], Michal Lehnert[c], Stevan Savić[d,*], Dragan Milošević[d]

[a] Institute of Computer Science of the Czech Academy of Sciences, 182 07, Prague 8, Czech Republic
[b] Global Change Research Institute of the Czech Academy of Sciences, 603 00, Brno, Czech Republic
[c] Department of Geography, Faculty of Science, Palacký University Olomouc, 771 46, Olomouc, Czech Republic
[d] Climatology and Hydrology Research Centre, Faculty of Sciences, University of Novi Sad, 21 000, Novi Sad, Serbia

ARTICLE INFO

Keywords:
Local climate zones
Surface urban heat island intensity
LANDSAT-8
Seasonality
Statistical analysis
Central Europe

ABSTRACT

This study analyzes inter- and intra-zonal seasonal variability of surface urban heat islands (SUHIs) within the methodological framework of local climate zones (LCZs) in three central European cities (Prague, Brno and Novi Sad). These cities differ in urban area and structure as well as in topography and hinterland land-cover features. LCZs were delineated on the basis of a GIS-based classification method. Land surface temperature (LST) was derived from LANDSAT-8 scenes in the period 2013–2018. The first step was to detect seasonal SUHI intensity differences for built LCZ types and LST for land-cover types of LCZ. The results revealed the highest differences in summer and spring, and lowest in winter. The highest SUHI intensity values occur in densely built-up and industrial zones, and the lowest in sparsely-built city outskirts. The coolest LCZs based on LST were dense trees and water areas in spring and summer. The second step aimed to analyze the effects of vegetation on SUHI formation. Hence, 11 land cover subclasses (from dense trees to bush/scrub) were defined in order to research intra-zonal seasonal LST variability. The height and density of vegetation have substantial effects on intra-zonal variability of LST in land-cover types of LCZ, whereas differences between forest subclasses were relatively low. Finally, the character of the vegetation had a substantial influence on intra-zonal LCZ variability of LST and SUHI formation. Further research in this field could contribute to better understanding of micro- and mezzo-climate-scale patterns, as well as better adaptation to climate change in urban areas.

1. Introduction

Urbanization is one of the main driving forces of landscape change in Europe [1]. The territory of urban agglomerations, including urban and suburban landscapes, constitutes an ever-increasingly important part of the surface [2]. Urban landscape is characterized by structures, arrangements and compositions of land cover distinctly different from those of rural or natural landscapes. Significant proportions of urban areas are covered with artificial – mostly impervious – surfaces, which substantially impact upon the thermal regime of the landscape and thus modify the climate of urban areas. Increased temperatures in such places may significantly alter many aspects of all kinds of life, including biodiversity [3,4], population health [5–8] and overall sustainability of urban areas [9,10]. Considering that global climate change has led to increases in summer climate indices in many urbanized regions, including central Europe [11–15], the importance of studying any additional heat load in urban areas at a local scale is currently of especially pressing importance.

Higher land surface temperatures (LSTs) in urban landscapes in comparison with surrounding (rural or natural) landscapes occur in particular response to lower albedo, higher degree of sealing and anthropogenic heat emission [16]. Compact areas of increased LST in urban areas give rise to a phenomenon known as the “surface urban heat island” (SUHI), something that has been the subject of many studies in recent decades [17–19]. Several investigations have demonstrated that the intensity and character of SUHI greatly influence the air temperature conditions of a city, contributing to the formation of UHIs – air-temperature-based urban heat islands [18–22]. However, the study of temperature differentiation between urban surfaces has long been limited to description of differences between urban, suburban and rural landscapes/areas [18]. This has reflected the comparatively low spatial resolution of the sensors used, as well as the absence of a

* Corresponding author. Climatology and Hydrology Research Centre, Faculty of Sciences, University of Novi Sad, Trg Dositeja Obradovića 3, 21 000, Novi Sad, Serbia.
E-mail addresses: geletic@cs.cas.cz (J. Geletič), stevan.savic@dgt.uns.ac.rs (S. Savić).

https://doi.org/10.1016/j.buildenv.2019.04.011
Received 20 December 2018; Received in revised form 10 March 2019; Accepted 4 April 2019
Available online 08 April 2019
0360-1323/ © 2019 Elsevier Ltd. All rights reserved.

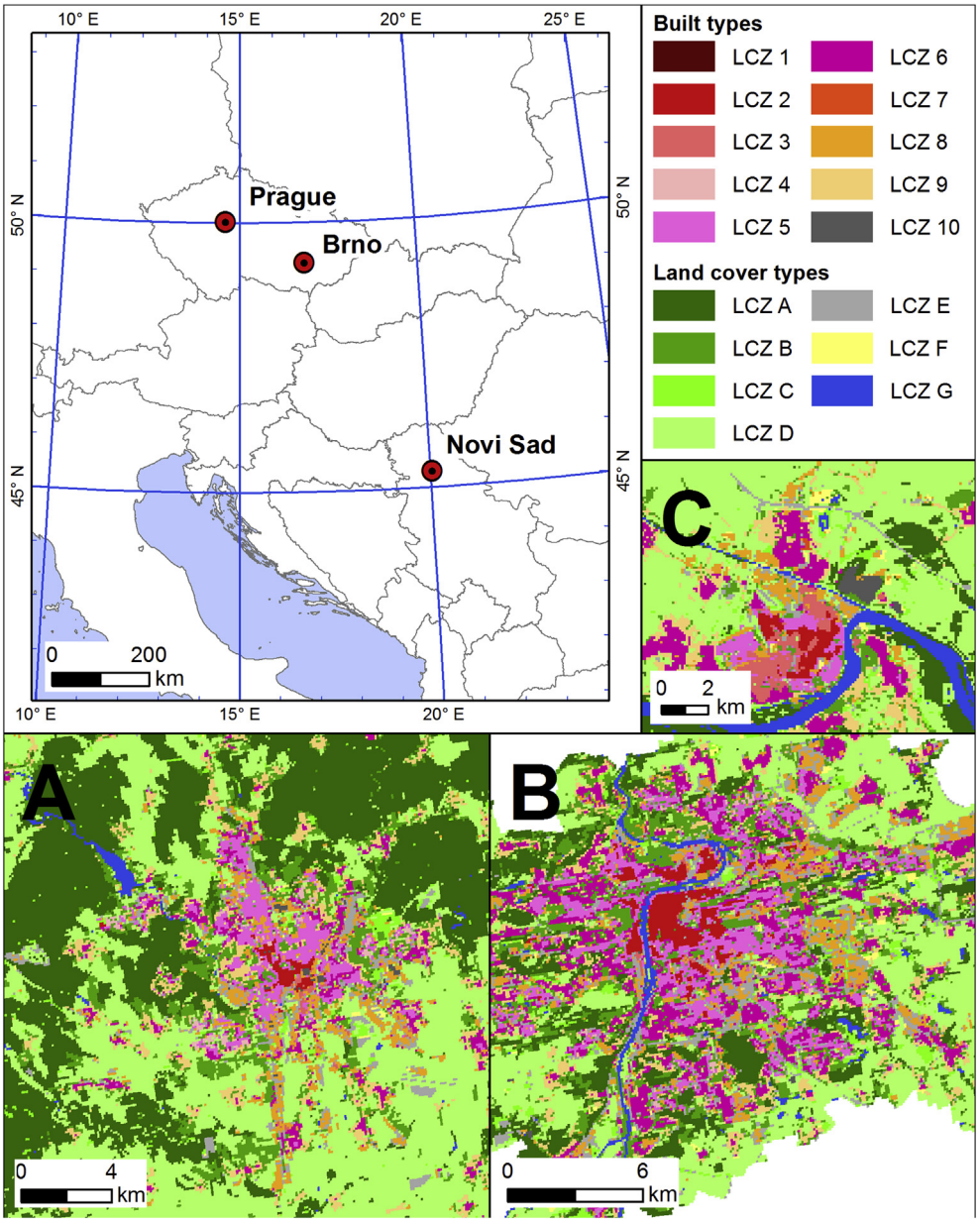

Fig. 1. Locations of the cities studied, indicating local climate zones in Brno (a), Prague (b; both Czech Republic) and Novi Sad (c; Serbia). See Appendix A for full names of built and land-cover LCZ types.

uniform and generally-recognized classification of urban cover/use types appropriate to LST analyses. Conventional land use/cover classifications, e.g. CORINE Land Cover [23] 500-m MODIS Land Cover Maps [24], USGS Global Land Cover [25] and GlobeLand30 [26] have not permitted discrimination within the diversity of the urban building environment, whereas urban landscape classification has not reacted to the climatic perspective of the urban landscape [27]. This apparent impasse has recently been resolved, at least in part, by classification based on the concept of local climatic zones (LCZs) [28].

LCZs consist of areas of uniform surface cover structure, material, and human activity. They may cover areas ranging from hundreds of meters to several kilometers on the horizontal scale. There are several advantages associated with the LCZ concept as an approach to analysis: it is a global classification scheme with a limited number of classes (10 built and 7 land-cover types) and these classes are defined by physical properties of the urban environment. Although LCZs were originally conceived for the study of air temperature in urban and suburban landscapes, based on an assumption that each LCZ has a generally unique building height and density, as well as some predominant types of building material (concrete, masonry, metal, glass, wood, etc.), that provide different emissivity, the concept was soon recognized as being particularly suitable for studying LST variation in the urban landscape.

Indeed, recent studies have confirmed assumptions of significant or substantial LST differences among LCZs [29–31].

With the adoption of the LCZ concept for LST/SUHI studies, however, further research perspectives and pending queries have emerged, including the effects of day period, seasonality and/or thermal anisotropy on LST variability in particular LCZs [30]. With respect to the results of studies analyzing air temperature variability in LCZs [13,32,33], it is natural to assume that times of day and seasons generate different effects on LST in given LCZs. Indeed, Geletič et al. [30] presented diurnal/nocturnal LST differences between LCZs in the city of Brno (Czech Republic) and Wang et al. [34] recently reported on diurnal/nocturnal LST differences between LCZs in Phoenix (Arizona) and Las Vegas (Nevada). Seasonal variations of LST among LCZs have been covered recently by Gémes et al. [35], who used a single scene for

February, May, July and September to express seasonal LST in LCZs in Szeged (Hungary). Further, Ziaul and Pal [36] presented figures from which seasonal variations in LST in the LCZs of English Bazar (India) may be identified.

While the first efforts to quantify seasonal variability of SUHI within the methodical framework of the LCZ concept are emerging, several studies have recently addressed seasonal variation in SUHI and/or seasonal differences of LST between land-cover/use in diverse world regions [37–44]. The sheer quantity and scope of the above contributions presumably demonstrate the existence and importance of seasonal effects in SUHI analyses.

Based on the review above, we assume that wider recognition and employment of the LCZ concept in studies addressing SUHI analyses help to standardize research and facilitate further progress towards more advanced knowledge of the influence of factors such as building structure and material or vegetation state and type down to micro–-mezzo-scale climate patterns.

Therefore, this study takes up the challenge of studying SUHI defined on the basis of LCZs and analyzing seasonal differences of LST among particular LCZs. More precisely, the aims of this study are to: i) investigate SUHI based on LCZs, ii) analyze seasonal variations of LST among LCZs and iii) analyze seasonal differences in the intra-zonal variability of LCZs A–C by imposing new subclasses, using the central European cities of Prague and Brno (Czech Republic) and Novi Sad (Serbia) as examples.

2. Study areas

In the Czech Republic, the study covers the two largest cities: Prague, the nation's capital and Brno, the regional capital of the eastern province of Moravia. It also takes in Novi Sad, the second-largest city in Serbia (Fig. 1; Table 1).

There are few marked differences in urban morphology and topography between the three cities. Brno and Prague both lie among hills. Their elevations range from under 200 m to over 500 m in Brno and under 200 m–400 m in Prague, while Novi Sad lies in the Pannonian Plain extension into northern Serbia (Vojvodina). Thus, the topography containing its built-up areas is quite gentle; elevations vary between 72 m and 80 m. Even the exceptions – the Petrovaradin and Sremska Kamenica districts – achieve only around 80–200 m.

The similarities in the history of the cities studied (especially Austro-Hungarian Empire architecture, socialist urbanization policy, and the loosely coordinated urbanism of the early post-socialist era) are clearly reflected in their growth, largely consisting of chronologically concentric areas of development (a distinct historical center, working outwards through residential buildings dating back one or two centuries or newly-constructed, industrial zones, high-rise and low rise estates, modern concentrations of retail outlets, quite extensive malls and city-sponsored gardening plots). This has led to neighborhoods with both irregular and regular (grid and radial grid) street plans being present in all cities. However, Prague and Novi Sad feature substantial, navigable rivers (the Vltava and the Danube respectively) while Brno's waterway (the Svitava) is comparatively insignificant. In Prague and Brno, larger areas of urban greenery (e.g. parks, gardens) are contained within the compact city than in Novi Sad. In contrast, it must also be noted that streets in Novi Sad are largely lined with trees, a phenomenon which is currently absent in Brno.

From the perspective of LCZs, the concentric patterns of the zones are particularly marked in Brno and Prague. In Novi Sad the concentric pattern is less developed; the zones tend to reflect the different functions of individual part of the city (Fig. 1). The area of LCZ 2 (compact midrise) in historical city centers is most developed and compact in Prague, whereas in Brno, and particularly in Novi Sad, more scattered nodes of LCZ 2 are observed. In Prague and Brno, LCZ 2 is clearly surrounded by LCZ 5 (open midrise), the most frequent type of development in both cities. In Novi Sad, a substantial part of the compact city is represented by LCZ 3 (compact low-rise), which is rare in Brno as well as in Prague (Appendix A). In all the cities there is an increase of areas classified as LCZ 6 (open low-rise) towards the outer boundaries of compact development. Areas of LCZ 6 are more frequent in Prague and Novi Sad, less so in Brno (Fig. 1, Appendix A). In Novi Sad, the industrial area (LCZ 10) is clearly organized in the north-east part of the city, while related areas of LCZ 8 (large low-rise) and E (bare rock or paved) are located along the canal. In contrast, LCZs 8, 10 and E in Brno and Prague appear especially on the outer part of the cities, or create ribbons of compact development in the countryside. In Brno, in particular, there are also significant patches of LCZ 8, 10 and E in the core areas of the city. Dispersed areas of LCZ 9 (sparsely built), in Brno and Prague mixed with areas of LCZ B (scattered trees), occur in all the cities at the boundary of compact urban development and hinterland. In Prague's and Novi Sad's surroundings, as in the landscape south of Brno, LCZ D (low plants) dominates, but to the north of Brno lie large areas of LCZ A (Fig. 1).

Considering the similarities in the history of the cities, construction materials used in particular urban neighborhoods (resp. LCZ) are much the same. The old town areas (particularly LCZ 2) and modern residential building blocks constructed in the last 30 years (particularly LCZ 2 in Novi Sad and LCZ 5 in Brno and Prague), consist largely of masonry material and roofs with red or dark tiles. Furthermore, buildings (mostly houses) in LCZs 3, 6 and 9 are also characterized by masonry material and tiles on the roofs. On the other hand, high- and mid-rise buildings are dominant in LCZ 4, constructed during the second half of the 20th century (the socialist period), with concrete material and flat roofs of concrete, or with an asphalt layer (leading to the consideration of lower building as high, especially in Brno and Prague, and therefore parts of this development being classified as LCZ 5). In commercial and industrial areas of LCZ 8 and 10, concrete construction materials and/or metal sheets with flat roofs are typical of all the all the studied cities.

Novi Sad lies in the Pannonian Plain extension into northern Serbia (Vojvodina). Thus, the relief containing its built-up areas is quite gentle; elevations vary between 72 m and 80 m. Even the exceptions – the Petrovaradin and Sremska Kamenica districts – achieve only around 80–200 m. Streets of moderate width serve as communications in the densely built-up central area, while avenues and boulevards link certain outlying parts of the city. The built-up part consists of mid-rise blocks (largely four to eight floors high), with a few of 16–18 stories, low-rise residential areas and some parks. The northern suburban zones contain much of the city's warehousing and light industry, intermixed here and there with low-rise residential housing. The banks of the River Danube

Table 1
Basic data and general climate features in Brno, Prague (Czech Republic) and Novi Sad (Serbia), for the reference period 1961–2000.

	Brno	Prague	Novi Sad
Basic data			
Size of study area [km]	25 × 25	35 × 25	20 × 17
Cadastral area [ha]	23,022	49,600	12,940
Number of inhabitants (city)*	377,800	1,285,500	332,300
Number of inhabitants (agglomeration)*	592,400	2,046,500	400,300
Mean elevation [m]	259	288	76
Latitude (city center)	49°12′N	50°05′N	45°15′N
Longitude (city center)	16°37′E	14°25′E	19°51′E
Climate features (1961–2000 reference period)			
Mean annual temperature [°C]	9.1	8.4	11.0
Highest mean monthly temperature [°C]	19.3	18.2	21.3
Lowest mean monthly temperature [°C]	−1.9	−1.4	−0.7
Mean annual amount of precipitation [mm]	505	526	597
Köppen's climate type [45]	Cfb	Cfb	Cfb

* Data for Czech Republic are valid to 2017, sourced from the Czech Statistical Office (https://www.czso.cz/csu/czso/home). Data for Novi Sad are valid to 2017, sourced from the Statistical Office of the Republic of Serbia (http://www.stat.gov.rs).

provide a “green avenue”, while more vegetation is concentrated in the parks and around the city's outskirts. Most of the linking avenues and boulevards, as well as the streets in densely built-up areas, feature mature trees (more than 30 years old) on both verges. This “green” accompaniment to the streets of Novi Sad is largely absent from the streets of Brno. The River Danube creates a division between the south and south-eastern urban areas of Novi Sad and the most built-up city areas. At his point, the width of the Danube is considerable, between 260 m and 680 m. The Danube-Tisza-Danube Canal, a narrow waterway, runs through the northern portion of the city. Largely agricultural land, featuring, low, cultivated plants, typifies the northern, western and eastern hinterlands. To the south lies Fruška Gora, a low mountain area around 80 km long east to west and 15 km from north to south, highest peak Crveni Čot at 539 m, with mixed forests consisting of various types of deciduous trees.

According to multi-decade period measurements (1961–2000) the air temperature and precipitation regimes in all three cities are relatively similar (Table 1).

3. Materials and methods

3.1. Local climate zones and subclasses

The landscape classification used herein consists of 17 standard LCZs, of which 15 are defined by surface structure and cover and two by construction materials and anthropogenic heat emissions. The standard set is divided into “built types” 1–10, and “land-cover types” A–G [28]. Contained within the specialist literature are approach methodologies to LCZ mapping based on: (1) manual [46], (2) GIS-based [47,48], (3) remote sensing [49] and (4) combined methodology [50,51]. Since the satellite imagery-based method relies partly on thermal bands and therefore should not be used for independent analyses of LSTs, the GIS-based method developed by Geletič and Lehnert [47] was employed for delineation of LCZs in this study. This relies on physical properties of the environment that are accurately measurable, combined with a decision-making algorithm that is clearly defined on the basis of inherent physical parameters, as defined by Stewart and Oke [28]. These include: (1) building surface fraction (BSF), (2) pervious surface fraction (PSF), (3) impervious surface fraction (ISF), and (4) height of roughness elements (HRE), complemented by (5) the number of buildings (NoB). The classification process consisted of dividing all the urban areas into grid cells of 100 × 100 m, each of them conforming to defined physical parameters [47]. Independent testing of the algorithm for defining percentage coverage for individual LCZs indicated close agreement with areas established through expert local knowledge (about 87% agreement in Brno, 89% in Prague and 90% in Novi Sad). The absolute and relative numbers of cells assigned to LCZs appear in Appendix A.

Stewart and Oke [28] maintained that land-cover types can be further classified by seasonal and/or ephemeral properties (i.e. bare trees, snow-covered ground, dry/wet ground). The first four classes, LCZ A–D, may be strongly affected by seasonality. For example, the climatic characteristics of broad-leaved, mixed and coniferous forests (generally LCZ A) are quite different. Similar complications exist in urban growth patterns, especially in LCZ B. There are differences within cities between densely-leaved parks, scattered trees, and botanical gardens with low trees and scrub. In order to lend some clarity to these differences, subclasses of LCZs A–C (Fig. 2) were established beyond the usual standards. LCZ A is very often a mixture of coniferous and broad-leaved trees. The main task was thus to define three general types for LCZ A: coniferous (*con*; LCZ A_{con}), mixed (*mix*; LCZ A_{mix}) and broad-leaved (*brl*; LCZ A_{brl}) forests. LCZs B and C both exist at differing densities and feature different growth patterns, so subclasses were delineated as: high-density (*den*; LCZ B_{den} and LCZ C_{den}); low-density and/or sparse patterns (*sce*; LCZ B_{sce} or LCZ C_{sce}); and isolated patches of growth (*iso*; LCZ B_{iso} or LCZ C_{iso}). Gardens with fruit trees were allocated their own subclass (*orc*; LCZ B_{orc}), as were vineyards and hop gardens (*vin*; LCZ B_{vin}). Absence of yearly data on crops in agricultural areas meant that LCZ D was not further subclassified. The absolute and relative number of cells allocated to subclasses in the cities studied appear in Appendix A.

3.2. Land surface temperature and SUHI

The records of the LANDSAT-8 satellite for the period from spring 2013 to summer 2018 were employed to establish LST. LANDSAT-8 has two thermal bands, Band 10 and Band 11 [52]. Data herein were atmospherically corrected using the Landsat 8 Surface Reflectance Code product (LaSRC) [53], providing per-pixel quality assessment flags. Only clear pixels were used in the current analysis. However, LANDSAT-8 does not provide data for surface emissivity calculation, so a land-surface emissivity (LSE) algorithm was used to estimate emissivity from the normalized difference vegetation index (NDVI) [54]. The approach to LANDSAT-8 scene processing is summarized in Appendix B. This study analyzed 80 scenes, all of them snow- and cloud-free; 19 for Brno, 32 for Prague and 29 for Novi Sad.

It is important to note that all temperature data in this study were analyzed and presented as differences between the mean LST value of a given LCZ (or subclass of LCZ) and the mean LST value of LCZ A (LCZ A DIF). For built types of LCZ, these values were further considered in terms of the SUHI intensity of the given LCZ [30].

3.3. Seasonality and intra/inter-zonal variability

Seasonality was analyzed in terms of meteorological seasons: winter (1 December to 28/29 February), spring (1 March to 31 May), summer (1 June to 31 August) and autumn (1 September to 30 November). Twelve scenes were analyzed in the winter season (4 in Brno, 5 in Prague and 3 in Novi Sad), 29 scenes in the spring season (11 in Brno, 12 in Prague and 6 in Novi Sad), 26 in the summer season (3 in Brno, 10 in Prague and 13 in Novi Sad) and 13 in the autumn season (1 in Brno, 5 in Prague and 7 in Novi Sad). The basics of each scene analyzed appear in Appendices C.1–3.

Based on the assumption that individual LCZs should exhibit certain features of typical LST regimes that may vary with the seasons [30], all scenes were divided by season and analyzed for LCZ inter-zonal variability (see Section 3.1). At the same time, it was assumed that individual LCZs exhibit certain intra-zonal variability, the extent of which differs with season [30] and that this (intra-zonal) variability may be partly explained by imposing subclasses.

Analysis of differences in LST between LCZ classes, and particular subclasses, (both based on LCZ A DIF) was undertaken by ANOVA [55]. In the interests of consistency, a careful assessment of the assumptions intrinsic to the application of ANOVA was made (normality testing with the Kolmogorov-Smirnov tests, Q-Q plots, and comparisons of LCZ surface temperature variability) [30]. When the one-way ANOVA F-test ($p < 0.001$) indicated significant differences in LST, the Tukey-HSD test was employed to reveal which pairs of LCZs were significantly differentiated in terms of their mean LST. All 80 scenes were analyzed individually in these terms. Finally, the score that totaled the tests indicating significant temperature differences was established for each LCZ. Interpretation of this score is straightforward: LCZ subclasses with higher scores are better differentiated from other zones in terms of their characteristic LSTs. Conversely, LCZ subclasses with lower scores are less distinguishable from other zones in terms of their characteristic LSTs.

4. Results

4.1. Seasonal differences of LST in LCZs – SUHI intensity

SUHI was not well developed in the winter season in a few cases. In Prague and Novi Sad, LCZ G – in both cities dominated by substantial

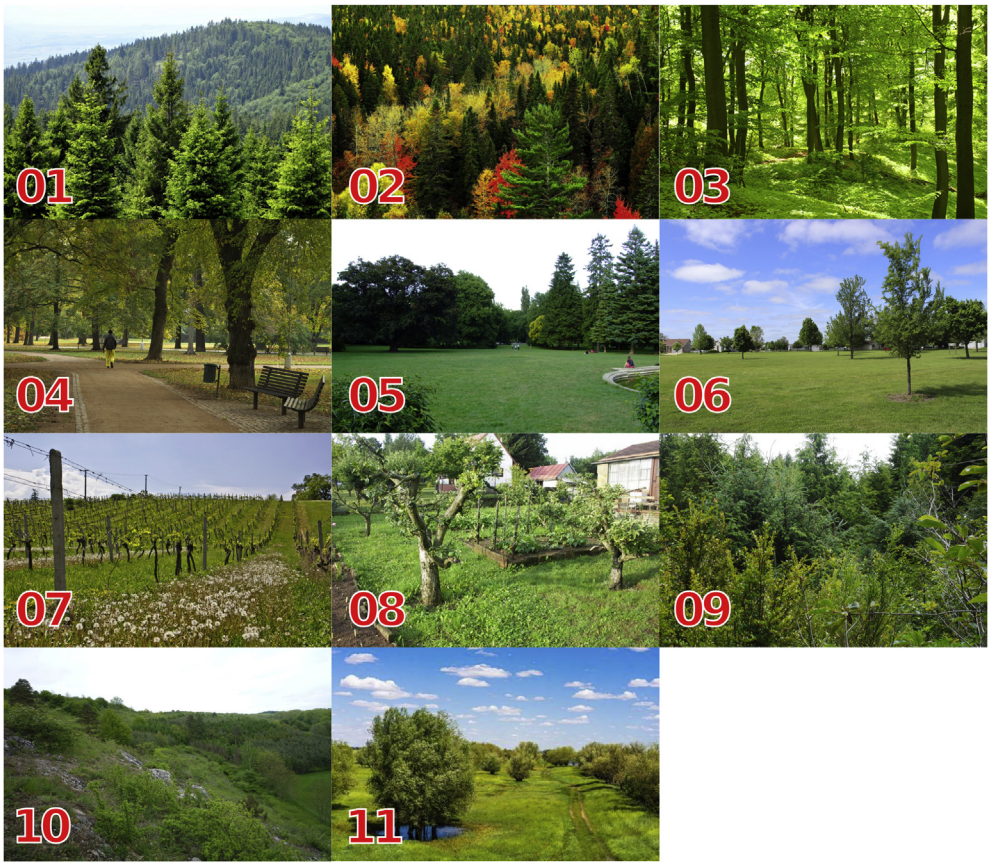

Fig. 2. Example of subclasses delineated within land-cover types of LCZ. The original LCZ class appears in brackets, followed by the recommended three-letter marking of subclass; 01 – coniferous forests (LCZ A; LCZ A_{con}), 02 – mixed forests (LCZ A; LCZ A_{mix}), 03 – broad-leaved forests (LCZ A; LCZ A_{brl}), 04 – densely-forested parks (LCZ B; LCZ B_{den}), 05 – low-density forested parks (LCZ B; LCZ B_{sce}), 06 – park with low and isolated, or scattered, trees (LCZ B; LCZ B_{iso}), 07 – vineyards and hop gardens (LCZ B; LCZ B_{vin}), 08 – gardens with low fruit trees (LCZ B; LCZ B_{orc}), 09 – dense bush/scrub (LCZ C; LCZ C_{den}), 10 – low-density or scattered bush/scrub (LCZ C; LCZ C_{sce}), 11 – isolated bush/scrub (LCZ C; LCZ C_{sce}).

rivers – was the warmest LCZ in the winter season. Further, in Novi Sad the mean LCZ A DIF of LCZ D was even higher than LCZ A DIF of all built LCZs ("SUHI"). In these cases, we cannot, therefore, strictly speaking, use SUHI in significant discussion. Further, in Novi Sad only small differences in LCZ A DIF among built types of LCZ appeared. A higher LCZ A DIF of built types of LCZs in comparison with land-cover LCZs was pronounced in Brno, where the hottest built types of LCZ were LCZ 2 (SUHI intensity 3.3 °C) and LCZ 10 (3.7 °C). In Prague, the hottest built types of LCZ were LCZ 2 (1.8 °C) and LCZ 3 (1.3 °C). In Brno and Prague, the lowest LSTs were similarly observed for LCZ A followed by LCZ D. In Novi Sad, the lowest LSTs were found for LCZ 4 and – unexpectedly – for LCZ 10 as well (LCZ A DIF –0.9 °C for both; Fig. 3). In winter, the LST differences among LCZs, and related SUHI intensity, stood at their least of all the seasons. Statistically significant differences between pairs of LCZs were more often found in Brno and Prague than in Novi Sad (Fig. 4).

In the spring season, differences started to become evident in LCZ A DIF among LCZs and related SUHI intensities. At the same time, interquartile ranges of LCZ A DIF and the number of outliers was higher than in the winter season for most of the LCZs (Fig. 3). Just as in the winter season, significant differences between pairs of LCZs were found particularly in Brno and Prague in the spring season (Fig. 4). In Brno, the highest LST was observed in LCZ 10, in which SUHI intensity reached 10.1 °C followed by LCZ 3 (8.8 °C) and LCZ 2 (8.6 °C). In Prague, the highest SUHI intensities were found for LCZ 3 (7.2 °C), LCZ 2 (6.4 °C) and LCZ 8 (5.9 °C). In Novi Sad the highest SUHIs were observed in LCZ 7 (7.2 °C) and LCZ 8 (6.4 °C). An only slightly lower SUHI emerged in LCZ D (6.0 °C). The lowest LSTs occurred in the spring season in all the cities observed for LCZ G, followed by LCZ A (Fig. 3).

In the summer season, differences in LCZ A DIF among LCZs and related SUHI intensity were generally at their highest. Significant differences in LST were disclosed for most pairs of LCZs in all the cities studied (Fig. 4). In Brno, the highest SUHI intensity was found in LCZ 10 (13.9 °C), the second highest in LCZ 3 (12.3 °C) and third for LCZ 2 (12.2 °C). In Prague, the highest SUHI intensity occurred in LCZ 3 (11.6 °C), followed by LCZ 2 (10.4 °C) and LCZ 8 (9.9 °C). In Novi Sad, the order of LCZs based on SUHI intensity ran from highest in LCZ 10 (10.9 °C), then LCZ 2 (10.8 °C), LCZ 8 (10.4 °C), to LCZ 3 (10.2 °C). In the summer season, as in the spring season, LCZ G and LCZ A emerged as the coolest in all the cities studied. Among built types of LCZ, the lowest temperatures were apparent in LCZ 9 in all the cities (Fig. 3).

In the autumn season, LST differences among LCZs and SUHI intensities were lower than in summer season. In Brno and Prague, LCZ A DIF between pairs of LCZs were significant in most cases, but for Novi Sad the differences were significant in only approximately half (Fig. 4). In Brno, the highest autumn SUHI intensity was observed for LCZ 10 (11.0 °C), then LCZ 3 (9.7 °C) followed by LCZ 2 (9.1 °C) and LCZ 8 (8.7 °C); it must be noted at this point that only one appropriate autumn image was available for Brno. In Prague, the highest SUHI intensities were found for LCZ 3 (4.5 °C), LCZ 2 and 8 (both 3.9 °C) and LCZ 10 (3.8 °C). In Novi Sad, the differences in SUHI intensity among the warmest LCZs were very low (LCZ 8 4.4 °C, LCZ 2 4.3 °C, LCZ 3 4.0 °C and LCZ 7 3.8 °C). The lowest LSTs in all the cities studied occurred in the autumn season for LCZ A. Among built-up types of LCZ, the lowest SUHI intensities were found for LCZ 9 (5.7 °C in Brno and 2.1 °C in Prague) and in Novi Sad for LCZ 4 (2.5 °C) (Fig. 3).

Comparing all the seasons in the cities studied, the SUHI differences were most pronounced in summer and were least marked in the winter season. In Brno and Prague, the temperature differences were generally more distinguishable than in Novi Sad. Regardless of differences in SUHI intensity among the cities and seasons, the higher LSTs were generally characteristic of LCZs 2, 3, 8 and 10.

Interpretation of the Tukey-HSD tests for all combinations of LCZ classes suggests thermal characteristics common to most of the LCZs throughout the cities and seasons. The robustness of this finding is confirmed by the high relative number of "hits" (significant differences

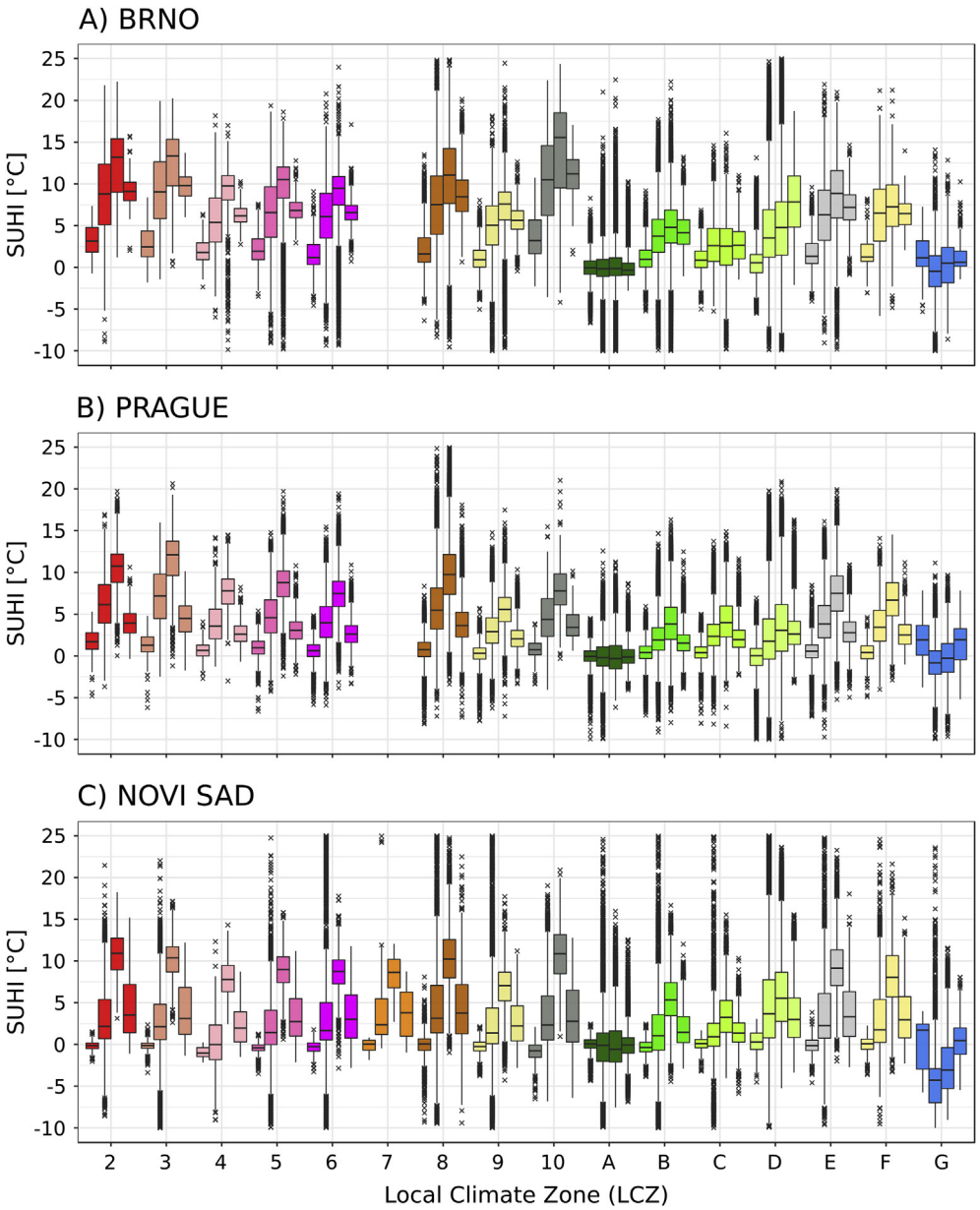

Fig. 3. Box-plots representing seasonal SUHI intensities in LCZ classes in Brno (a), Prague (b; both in the Czech Republic) and Novi Sad (c; Serbia); Left to right, the first box-plot is for the winter season, the second for spring, the third for summer and the fourth for the autumn.

in LST between pairs of LCZ, p-value < 0.05) in the average of all scenes analyzed (86.1% for Brno, 84.6% for Prague and 70.6% for Novi Sad) and similarities in the seasonal trends for the number of "hits" in these cities. The highest relative number of "hits" occurred in the summer season, at an overall average of 83.3% (86.0% for Brno, 88.4% for Prague and 75.5% for Novi Sad). The lowest values were in winter, at an overall average of 75.0% (84.8% for Brno, 76.2% for Prague and 64.2% for Novi Sad) (Appendix D.1).

4.2. Seasonal LST differences in subclasses

In Prague and Brno, 10 LCZ subclasses were identified, and 8 in Novi Sad. In all three cities, the smallest differences between seasons occurred in LCZ A subclasses. Generally, seasonal differences are expressed more definitely from LCZ B_{sce} to LCZ C subclasses (Fig. 5). Statistically significant differences in LCZ A DIF among subclasses were highest in summer and spring and lower in the winter season (Fig. 6).

LCZ A DIF differences were small among land-cover subclasses in all cities in the winter period. The minima were disclosed for Brno and Prague in LCZ A_{con} (−0.4 °C and −0.3 °C respectively), and LCZ A_{mix} (−1.7 °C) for Novi Sad. Very close values emerged for the Czech cities in LCZ A_{mix} −0.3 °C for both) and A_{brl} (0.1 °C); the Novi Sad figure for LCZ_{brl} was 0.0 °C. The highest LCZ A DIF values in Prague was in LCZ B_{vin} (2.3 °C), followed by Brno in LCZs B_{den} (1.5 °C) and B_{sce} (1.4 °C), and then Novi Sad C_{den} (0.1 °C) and B_{orc} (0.1 °C) (Fig. 5). Pairs of LCZ subclasses exhibited statistically significant differences in most cases in all the cities, but LCZs B_{orc} and C_{sce} showed more similarities with other subclasses (Fig. 6).

In the spring season, lower differences in LCZ A DIF in all cities were revealed in LCZ A subclasses, except for LCZ A_{brl} in Novi Sad, where the SUHI was lower only in comparison with LCZ B_{den} (−1.8 °C), which presents the maximum. In Czech cities the maximum LCZ A DIF values were recorded in LCZ B_{vin} (6.0 °C in Brno and 5.4 °C in Prague). In general, the spring values of LCZ A DIF were lower from LCZ C subclasses and LCZ B_{iso} to LCZ B_{den} (Fig. 5). Most cases were statistically significant, and in Brno all cases showed statistically significant

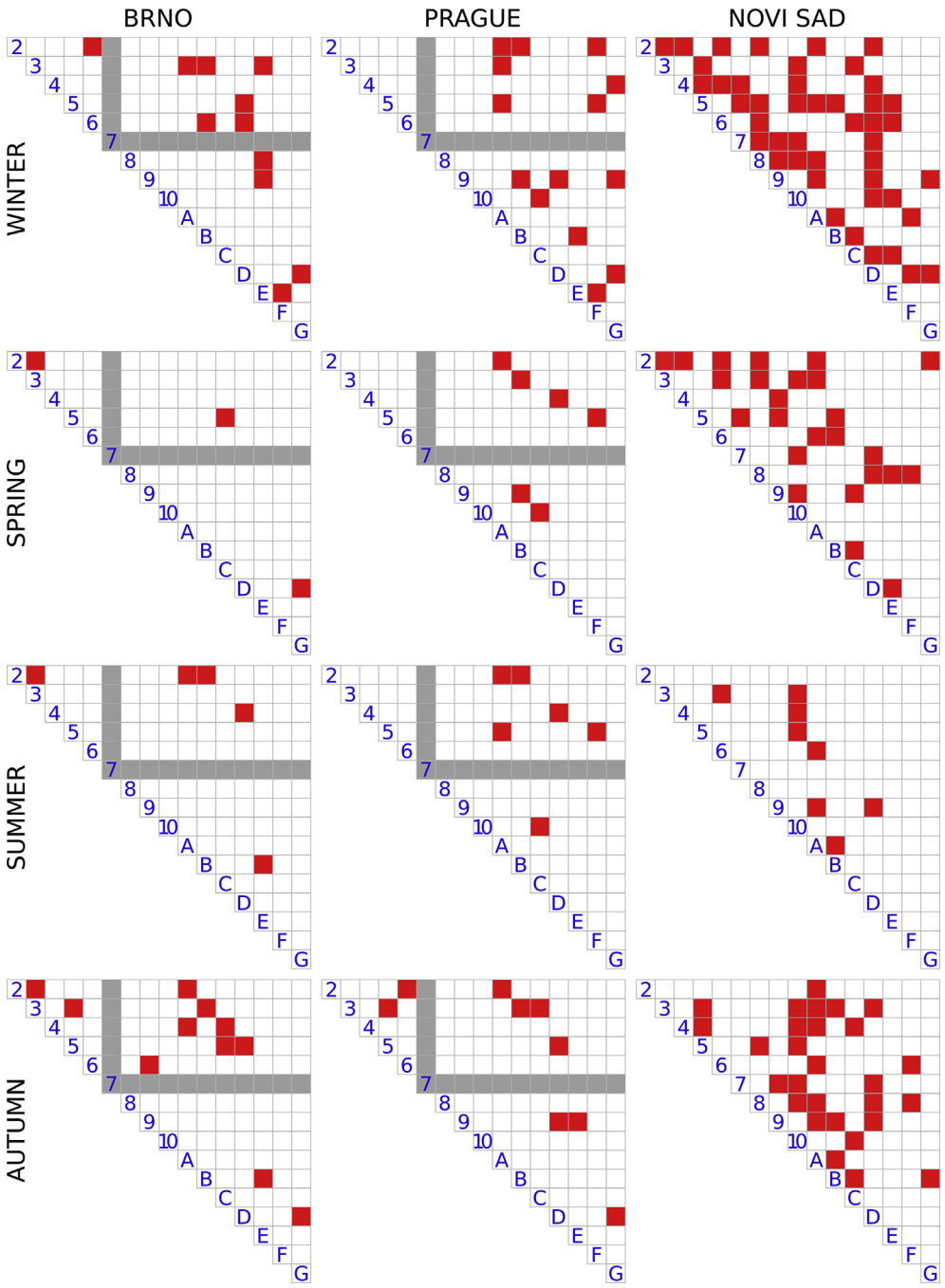

Fig. 4. Tukey-HSD test tests for all combinations of LCZ classes (blue numbers and letters) during the seasons for all three cities: white cells indicate LCZs pairs where average SUHI intensities are significantly different, red cells represent pairs of LCZs for which differences in SUHI intensities are insignificantly different and grey cells are empty or non-representative classes. (For interpretation of the references to color in this figure legend, the reader is referred to the Web version of this article.)

differences among subclasses (Fig. 6).

Differences in LCZ A DIF among LCZ land-cover subclasses were generally at their highest in the summer season. In Brno and Prague, the maximum LST was in LCZ B_{vin} (6.1 °C in Brno and 7.4 °C in Prague); in Novi Sad LCZ A DIF was highest in LCZ B_{iso} (6.1 °C). Furthermore, high values were evident in LCZ B_{iso} (Prague 6.3 °C, Brno 6.0 °C), C_{sce} (Prague 4.5 °C, Brno 2.7 °C, Novi Sad 5.1 °C) and LCZ B_{sce} (Prague 3.6 °C, Brno 5.4C, Novi Sad 5.1 °C). Interestingly, quite a high LCZ A DIF value emerged in LCZ A_{mix} (2.6 °C) in Novi Sad (Fig. 5). In only very few pairs of LCZ subclasses were differences in LCZ A DIF values statistically insignificant for the summer period: Prague one case, Brno three cases, and Novi Sad five cases (Fig. 6).

In autumn, the seasonal differences in LCZ A DIF were lower than in summer and spring, but higher than for the winter season. Minimum LCZ A DIF values occurred in LCZ A_{con} (Prague −0.7 °C, Brno −0.4 °C) and LCZ A_{mix} (−0.1 °C) in Novi Sad. In the Czech cities, the maximum SUHI emerged in B_{vin} (6.4 °C in Brno and 3.3 °C in Prague), while for Novi Sad the highest LCZ A DIF was for LCZ B_{orc} (2.4 °C). Intensities in Brno (4.3 °C) and Prague (1.7 °C) were similar. Tests of statistical significance showed similar results as for the summer period, and most of the LCZ subclass pairs exhibit significant differences in LST (Fig. 6).

Finally, the subclasses disclosed characteristic surface temperatures that differed from those of other subclasses. The robustness of this finding was further confirmed by the fact that the relative number of

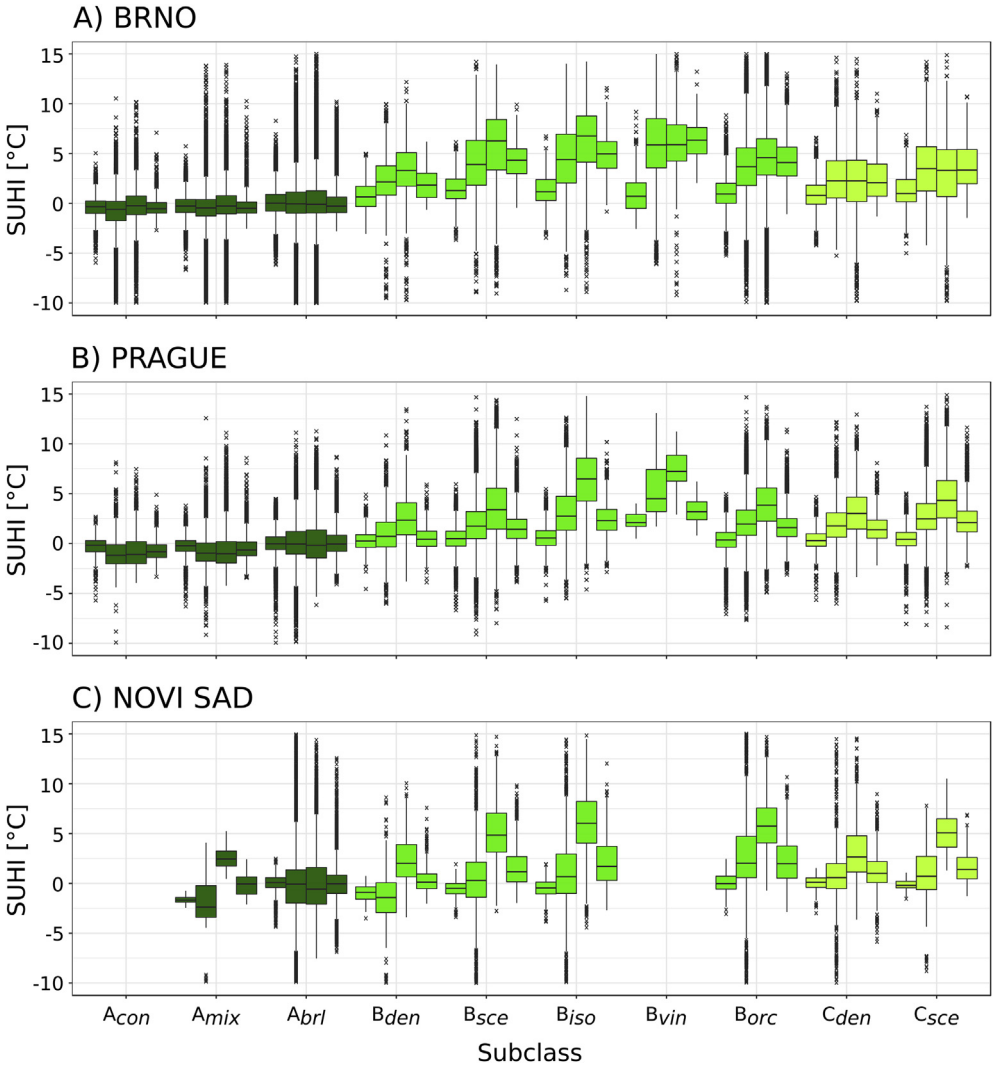

Fig. 5. Box-plots with seasonal LCZ A DIF in subclasses in Brno (A), Prague (B; both in the Czech Republic) and Novi Sad (C; Serbia); the line within the box indicates the median. The bottom of the box is the first quartile, and the top is the third quartile. Whiskers indicate the lowest value still within 1.5 IQR (IQR = third quartile − first quartile) and the highest value still within 1.5 IQR. Black crosses show outliers. From left to right, the first box-plot is for the winter season, the second for spring, the third for summer and the fourth for autumn.

"hits" for all the scenes analyzed was comparable for all three cities (86.1% for Brno, 87.0% for Prague and 65.8% for Novi Sad). The highest relative number of "hits" occurred, like those of LCZs, in the summer season, overall average 81.6% (88.1% for Brno, 89.8% for Prague and 66.8% for Novi Sad). The lowest values were in winter, overall average 75.4% (77.2% for Brno, 78.7% for Prague and 70.2% for Novi Sad). Surprisingly enough, the winter value was the highest of all seasons in Novi Sad (Appendix D.2).

5. Discussion

The results of this study raise several important points and pending issues in SUHI analyses, as well as in the concept of Local Climate Zones, that should be discussed further. However, the advantages and disadvantages of the methods employed herein the must be given careful consideration before any further elaboration.

5.1. Limits of the LST/LCZ-based study

Obtaining satellite data at high resolution at periodical intervals is very difficult, largely because of weather conditions. For analyzing LCZs in local patterns, scenes at a maximum resolution of 200 m are required; in practical terms, this leaves only two possibilities: ASTER and LANDSAT-8. ASTER is available for only a few scenes for each city, so LANDSAT-8 scenes were used. The main limitation of the study is that the times at which LANDSAT-8 measurements are taken are fixed. In all three cities, these times are between 9.30 and 10.00 UTC, which might appear a less than appropriate period for UHI analysis. However, SUHI differs from UHI [18] and may be considered as one of the factors determining – especially through surface-air turbulent fluxes – subsequent and more complex UHI formation. Therefore, earlier daytime measurements may well prove adequate for SUHI analysis too. In addition to the limited number of LANDSAT-8 scenes with appropriate weather conditions, the research was limited by different numbers of scenes for each season. Nevertheless, based on recommendations from previous research, the seasonality was studied on the basis of multiple years (2013–2018) in order to obtain more robust results [40].

Further, when analyzing SUHI, allowances must be made for the fact that LST is also strongly influenced by topography, especially in forested areas in high mountains [56]. In the course of interpretation of LST in forested areas, it is essential to bear in mind that calculations are limited to the tops of the tree crowns and, perforce, must neglect the surface temperature within the forest. It should be therefore be anticipated that overall forest surface temperature is lower than the data

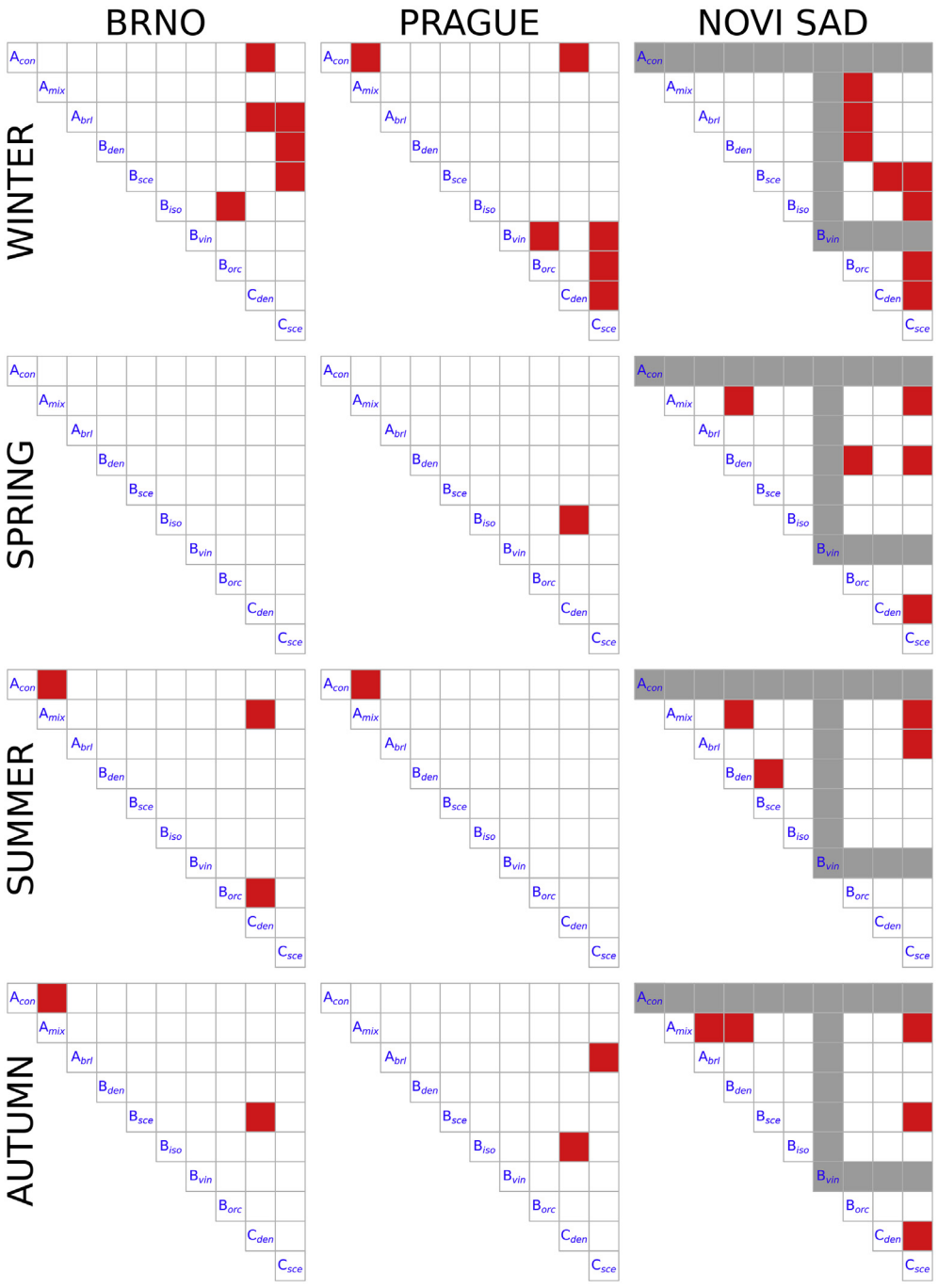

Fig. 6. Results of the Tukey-HSD test for all combinations of subclasses (subscript blue letters) during seasons for the three cities analyzed; red cells indicate pairs of LCZs for which LCZ A DIF are not significantly different (p-value > 0.05), while empty cells denote LCZs pairs for which average LCZ A DIFs are significantly different (p-value < 0.05). Grey cells are empty or non-representative ($n < 5$) classes. (For interpretation of the references to color in this figure legend, the reader is referred to the Web version of this article.)

shows, particularly in coniferous and mixed forests [57]. Similarly, in built-up areas with increasing proportions of vertically-oriented surfaces (building-height: width ratio) the effects of thermal anisotropy are more pronounced [58]. Consequently, differences in total surface temperature in urban areas may appear more marked than in rural areas in terms of the surface temperature as viewed by the sensor. The effects of all those factors also vary with season, since there are important changes in surface insolation during the course of the year [37,59,60].

Other limitations of the study associated with the LCZ concept arise largely out of its universal nature (neglecting regionally-specific features, settings of the intervals by physical properties, matters difficult to measure with sufficient accuracy resulting in weak reflections of thermal properties of building materials, etc.). Most of those limitations have been described in detail in previous studies [30,47]. Finally, the seasonality in LST variability of the LCZs described in this study may substantially complicate the temporal validity of LCZ classifications, particularly those based on satellite imagery methods [49,61]. This problem has already been recognized and reflected upon [62].

5.2. Discussion on SUHI patterns based on LCZs

The results of this study showed that in the three cities analyzed the highest LST/SUHI intensities are generally in LCZs 2, 3, 7, 8 and 10, i.e. in compact mid-rise and low-rise areas, as well as in the industrial zone. The lowest LST/SUHI intensities among the built-up areas emerged for LCZ 9. Including land-cover types of LCZ, the lowest LSTs were found for LCZ A. This corresponds with the findings of previous research in the Czech Republic [30,63] and other cities [29,64]. Most of these studies were; however, undertaken during the vegetation period. Detailed insight into seasonal differences provided by this study is derived from more comprehensive results.

The results of the analyses herein clearly indicate that LST differences among LCZs and related SUHI intensity in central European cities are notably dependent on seasonal periods (Figs. 3 and 4). The highest differences in LST/SUHI intensities between built-up/land-cover classes are typical for the spring and summer periods. Similar conclusions were reached for Beijing [40] Shenzhen [44], Hangzhou [65] and Tehran [41]. In contrast, considering less pronounced LST/SUHI intensities, the extent of heating in land-cover surfaces (LCZs A − D) during the non-vegetation period is similar to that on the outskirts of built-up types (LCZs 6, 7 and 9), or even similar to densely built-up areas (LCZs 2 and 3).

In Novi Sad, such statistically insignificant differences among LCZs were more pronounced than in Prague and Brno. There may be a range of reasons related to building materials, urban characteristics, the size of the urban space, its topography, and local and/or regional climate. The urban area of Novi Sad is smaller than that of Brno, and particularly that of Prague, and certain LCZs, such as 4, 5, 6 and 9 are scattered and non-homogeneous. Further, the relatively higher LST of LCZ D, resulting in several insignificant LST differences with other LCZs in winter, spring and autumn (mostly in early spring and late autumn) seasons, i.e. during non-vegetation periods, is explainable in Novi Sad by the local specific of particularly dark soil with low albedo (partially uncovered outside the vegetation period). Similar results were described by Wang and Huang [40] in the case of grassland in the urban area of Beijing (China). Furthermore, the effect of water areas on LST in other LCZs is as yet unclear, particularly in winter and spring when the LST values are highest in LCZ G (Fig. 3). According to the LCZ classification method deployed herein, more than 7% of the urban and hinterland areas of Novi Sad are classified as LCZ G, and the wide flow of the River Danube directly influences LCZs 2, 3, 4 and 5. Clarification of the direct seasonal influence of flowing water on densely built-up areas remains a challenge for future investigation. It has been indicated that the size and number of areas of water may have significant effects on LST [66]. According to a statistical analysis for Wuhan [67], the proportion of water body has a negative correlation with mean LST (lower ratio of water body leading to higher LST. Furthermore, research into the effects of the River Thames on urban surroundings has shown that airflow along rivers and canals may have a thermal influence on urban surfaces in the immediate vicinity [68].

5.3. Discussion of LST patterns in subclasses

Turning to subclasses of land-cover types of LCZ, the highest LST values among vegetated areas of LCZs A, B and C in all three cities studied were found in locations with isolated trees (LCZ B_{iso}) and gardens or orchard areas (LCZ B_{orc}) (Fig. 5). The latter two LCZ subclasses are similar to LCZ D, especially during the vegetation period, since their plant patterns are similar to those of some types of agricultural growth (for instance clover or soya to grass in LCZ B_{iso} or vegetables in gardens to maize or sunflowers, apple orchards, etc.). These similarities in vegetation could affect surface heating intensity, albedo values and shadow effects. LCZ subclasses with more trees (LCZ B_{den} and B_{sce}) and dense scrub (LCZ C_{den} and C_{sce}) exhibit lower summer and spring LST values. Obviously, the shadows cast by trees and scrub, darkness of surface coloration, and direct radiation are the main influences on seasonal LST variability. The lowest LST values of all are typical of forested areas (LCZs A_{con}, A_{mix} and A_{brl}).

The LST differences between land-cover LCZ subclasses depend heavily on seasonality, i.e. temporal differences in vegetation [64] and types of plants (low or high). The differences between LCZ A subclasses and other LCZs are at their highest in the summer period. Several factors serve to explain this: i) differences in radiation intensity; ii) enhanced evapotranspiration processes – when the air temperature exceeds 25 °C, most of the deciduous trees in a temperate climate initiate evapotranspiration; iii) higher albedo of tree crowns during the vegetation period; and iv) more shade from leaves during the vegetation period [69,70]. LCZs A_{con} and A_{brl} have higher albedo and accumulate less heat during daytime compared with less tree-dense subclasses. Based on research for western European cities [71], Poland [21] and the USA [72], deciduous and mixed trees reduce UHI/SUHI magnitude more strongly in comparison with coniferous forest. Importantly, results from the current study do not show substantial differences in LST between different types of forest. One of the reasons for this may be that most of the above studies centre around air temperature rather than LST. A second reason may be found in bias arising out of the location of coniferous trees (LCZs A_{con}) in generally cooler areas (e.g., less insolated valleys). By whatever means, vegetation reduces temperature during the summer months [73,74], leading to more comfortable open urban spaces [75–77]. According to a number of studies [78–81], decreases in air temperature from 1 °C to 7 °C may occur in the vicinity of large, deciduous wooded parks that include a river, and one large green patch has a stronger effect than several smaller patches.

6. Conclusions

Urban areas of Prague, Brno (Czech Republic) and Novi Sad (Serbia) and their hinterlands were classified in terms of LCZs and subsequently analyses were performed as to their seasonal SUHI variability. On the assumption that SUHI patterns are strongly influenced by different vegetation situations, additional LCZ subclasses were delineated for three land-cover zones (LCZs A − C). The additional classification system had 11 subclasses, and 10 of them were delineated in the three cities analyzed.

Regardless of the limitations inherent in temporal analysis, the research based on remote sensing data (using LANDSAT-8) provided valuable spatial analysis at quite high resolution. The results show that SUHI differences based on LCZs, as well as LST differences between land-cover subclasses, were most pronounced in summer, and that the minimum differences appeared in the winter period. It became clear that subclasses with fewer trees, such as LCZs B_{orc} and B_{iso}, have higher LSTs than subclasses with more trees and scrub (LCZs B_{sce}, B_{den}, C_{sce}, C_{den}), and much higher LSTs than densely forested areas (LCZs A_{con}, A_{mix}, A_{brl}). Finally, it should be noted that taller plants (mainly woody) have strong impacts on seasonal SUHI variability.

Whereas we performed detailed analyses of role of vegetation in LST/SUHI and its seasonal variability in this study, fuller understanding of the variability of LST/SUHI in LCZs requires further studies focusing on the influence of building height, density structure (texture) and material on LST differences between LCZs and intra-zonal variability in built-up types of LCZ. Altogether, results achieved by a coherent methodical framework, reproducible worldwide, can substantially contribute to better understanding of micro- and mezzo-climate-scale patterns, as well as better adaptation to climate change in urban areas.

Acknowledgements

This work was supported by the Ministry of Education, Youth and Sports of the Czech Republic within the National Sustainability Program I (NPU I), grant reference LO1415 and with institutional support, ref. RVO: 67985807. A partial contribution was made by the

Ministry of Education, Science and Technological Development of the Republic of Serbia through project no. 176020. This work was supported by an internal grant from Palacký University, Olomouc ref. IGA_PrF_2018_018 “Regions and Cities: Analysis of Development and Transformation”. The ERASMUS + exchange program contributed in creating the multinational research team that worked on this study, through staff exchange scholarships between Masaryk University in Brno, Palacký University in Olomouc (Czech Republic) and the University of Novi Sad (Republic of Serbia). Tony Long (Svinošice) helped work up the English.

Appendix A. Supplementary data

Supplementary data to this article can be found online at https://doi.org/10.1016/j.buildenv.2019.04.011.

Abbreviations

ANOVA	Analysis of variance
LCZ	Local climate zone
LCZ A DIF	Difference of mean LST between LCZ subclass and LCZ A
LST	Land surface temperature
SUHI	Surface urban heat island
USGS	United States Geological Survey

References

[1] M. Antrop, Landscape change and the urbanization process in Europe, Landsc. Urban Plann. 67 (2004) 9–26, https://doi.org/10.1016/S0169-2046(03)00026-4.
[2] European Space agency (ESA), Land Cover CCI: Product User Guide (Version 2.0), (2014) http://maps.elie.ucl.ac.be/CCI/viewer/download/ESACCI-LC-Ph2-PUGv2_2.0.pdf , Accessed date: 20 September 2018.
[3] K.J. Schmidt, H.H. Poppendieck, K. Jensen, Effects of urban structure on plant species richness in a large European city, Urban Ecosyst. 17 (2014) 427–444, https://doi.org/10.1007/s11252-013-0319-y.
[4] N. Čepelová, V. Kalusová, Z. Lososová, Effects of settlement size, urban heat island and habitat type on urban plant biodiversity, Landsc. Urban Plann. 159 (2017) 15–22, https://doi.org/10.1016/j.landurbplan.2016.11.004.
[5] R.S. Kovats, S. Hajat, Heat stress and public health: a critical review, Annu. Rev. Public Health 29 (2008) 41–55 https://doi:10.1146/annurev.publhealth.29.020907.090843.
[6] J. Tan, Y. Zheng, X. Tang, C. Guo, L. Li, G. Song, X. Zhen, D. Yuan, A.J. Kalkstein, F. Li, H. Chen, The urban heat island and its impact on heat waves and human health in Shanghai, Int. J. Biometeorol. 54 (2010) 75–84, https://doi.org/10.1007/s00484-009-0256-x.
[7] K.M. Gabriel, W.R. Endlicher, Urban and rural mortality rates during heat waves in Berlin and Brandenburg, Germany, Environ. Pollut. 159 (2011) 2044–2050, https://doi.org/10.1016/j.envpol.2011.01.016.
[8] S. Savić, V. Marković, I. Šećerov, D. Pavić, D. Arsenović, D. Milošević, D. Dolinaj, I. Nagy, M. Pantelić, Heat wave risk assessment and mapping in urban areas: case study for a midsized Central European city, Novi Sad (Serbia), Nat. Hazards 91 (2018) 891–911, https://doi.org/10.1007/s11069-017-3160-4.
[9] C.S.B. Grimmond, M. Roth, T.R. Oke, Y.C. Au, M. Best, R. Betts, G. Carmichael, H. Cleugh, W. Dabberdt, R. Emmanuel, E. Freitas, K. Fortuniak, S. Hanna, L.S. Klein, C.H. Liu, A. Nickson, D. Pearlmutter, D. Sailor, J. Voogt, Climate and more sustainable cities: climate information for improved planning and management of cities (producers/capabilities perspective), Proc. Environ. Sci. 1 (2010) 247–274, https://doi.org/10.1016/j.proenv.2010.09.016.
[10] Q. Huang, Y. Lu, Urban heat island research from 1991 to 2015: a bibliometric analysis, Theor. Appl. Climatol. 131 (2018) 1055–1068, https://doi.org/10.1007/s00704-016-2025-1.
[11] E. Lélovićs, J. Unger, S. Savić, T. Gál, D. Milošević, Á. Gulyás, V. Marković, D. Arsenović, C.V. Gál, Intra-urban temperature observations in two Central European cities: a summer study, Idojaras 120 (2016) 283–300.
[12] P. Štěpánek, P. Zahradníček, A. Farda, P. Skalák, M. Trnka, J. Meitner, K. Rajdl, Projection of drought-inducing climate conditions in the Czech Republic according to Euro-CORDEX models, Clim. Res. 70 (2016) 179–193, https://doi.org/10.3354/cr01424.
[13] N. Skarbit, I.D. Stewart, J. Unger, T. Gál, Employing an urban meteorological network to monitor air temperature conditions in the ‘local climate zones’ of Szeged, Hungary, Int. J. Climatol. 37 (2017) 582–596, https://doi.org/10.1002/joc.5023.
[14] O. Lhotka, J. Kyselý, A. Farda, Climate change scenarios of heat waves in Central Europe and their uncertainties, Theor. Appl. Climatol. 131 (2018) 1043–1054, https://doi.org/10.1007/s00704-016-2031-3.
[15] J. Geletič, M. Lehnert, P. Dobrovolný, M. Žuvela-Aloise, Spatial modeling of summer climate indices based on local climate zones: expected changes in the future climate of Brno, Czech Republic, Clim. Change (2019), https://doi.org/10.1007/s10584-018-2353-5.
[16] T.R. Oke, The energetic basis of the urban heat island, Q. J. Roy. Meteorol. Soc. 108 (1982) 1–24.
[17] M. Roth, T.R. Oke, W.J. Emery, Satellite-derived urban heat islands from three coastal cities and the utilization of such data in urban climatology, Int. J. Remote Sens. 10 (1989) 1699–1720.
[18] J.A. Voogt, T.R. Oke, Thermal remote sensing of urban climates, Remote Sens. Environ. 86 (2003) 370–384, https://doi.org/10.1016/S0034-4257(03)00079-8.
[19] S. Peng, S. Piao, P. Ciais, P. Friedlingstein, C. Ottle, F.M. Bréon, H. Nan, L. Zhou, R.B. Myneni, Surface urban heat island across 419 global big cities, Environ. Sci. Technol. 46 (2012) 696–703, https://doi.org/10.1021/es2030438.
[20] N. Schwarz, U. Schlink, U. Franck, K. Großmann, Relationship of land surface and air temperatures and its implications for quantifying urban heat island indicators - an application for the city of Leipzig (Germany), Ecol. Indicat. 18 (2012) 693–704, https://doi.org/10.1016/j.ecolind.2012.01.001.
[21] A. Majkowska, L. Kolendowicz, M. Półrolniczak, J. Hauke, B. Czernecki, The urban heat island in the city of Poznań as derived from Landsat 5 TM, Theor. Appl. Climatol. 128 (2017) 769–783, https://doi.org/10.1007/s00704-016-1737-6.
[22] B. Zhou, D. Rybski, J.P. Kropp, The role of city size and urban form in the surface urban heat island, Sci. Rep-UK 7 (2017) 4791, https://doi.org/10.1038/s41598-017-04242-2.
[23] European Environment Agency (EEA), CORINE Land Cover (CLC) 2012, Version 18.5.1, (2018) https://land.copernicus.eu/pan-european/corine-land-cover/clc-2012?tab=metadata , Accessed date: 20 September 2018.
[24] M.A. Friedl, D. Sulla-Menashe, B. Tan, A. Schneider, N. Ramankutty, A. Sibley, X. Huang, MODIS Collection 5 Global Land Cover: Algorithm Refinements and Characterization of New Datasets, 2001-2012, Collection 5.1 IGBP Land Cover, Boston University, Boston, MA, USA, 2010.
[25] B. Pengra, J. Long, D. Dahal, S.V. Stehman, T.R. Loveland, A global reference database from very high resolution commercial satellite data and methodology for application to Landsat derived 30m continuous field tree cover data, Remote Sens. Environ. 165 (2015) 234–248, https://doi.org/10.1016/j.rse.2015.01.018.
[26] J. Chen, Y. Ban, S. Li, China: open access to Earth land-cover map, Nature 514 (2014) 434, https://doi.org/10.1038/514434d.
[27] Copernicus, Mapping Guide for a European Urban Atlas (Version 4.7), (2018) https://land.copernicus.eu/user-corner/technical-library/urban-atlas-2012-mapping-guide-new , Accessed date: 20 September 2018.
[28] I.D. Stewart, T.R. Oke, Local Climate Zones for urban temperature studies, Bull. Am. Meteorol. Soc. 93 (2012) 1879–1900, https://doi.org/10.1175/BAMS-D-11-00019.1.
[29] N. Skarbit, T. Gál, J. Unger, Airborne surface temperature differences of the different local climate zones in the urban area of a medium sized city, Proceedings of the 2015 Joint Urban Remote Sensing Event, JURSE, Lausanne, Switzerland, 2015, pp. 1–4.
[30] J. Geletič, M. Lehnert, P. Dobrovolný, Land surface temperature differences within local climate zones, based on two central European cities, Remote Sens-BASEL 8 (2016) 788, https://doi.org/10.3390/rs8100788.
[31] Y. Wang, Q. Zhan, W. Ouyang, Impact of urban climate landscape patterns on land surface temperature in Wuhan, China, Sustainability-BASEL 9 (2017) 1700, https://doi.org/10.3390/su9101700.
[32] N. Müller, W. Kuttler, A.B. Barlag, Counteracting urban climate change: adaptation measures and their effect on thermal comfort, Theor. Appl. Climatol. 115 (2014) 243–257, https://doi.org/10.1007/s00704-013-0890-4.
[33] J.A. Quanz, S. Ulrich, D. Fenner, A. Holtmann, J. Eimermacher, Micro-scale variability of air temperature within a local climate zone in Berlin, Germany, during summer, Climate 6 (2018) 5, https://doi.org/10.3390/cli6010005.
[34] C. Wang, S.W. Myint, A. Middel, S. Kaplan, A. Brazel, J. Lukasczyk, Assessing local climate zones in arid cities: the case of Phoenix, Arizona and Las Vegas, Nevada, AGG Annual Meeting 2018 - New Orleans, USA, April 10-14, 2018.
[35] O. Gémes, Z. Tobak, B. van Leeuwen, Satellite based analysis of surface urban heat island intensity, J. Environ. Geogr. 9 (2016) 23–30, https://doi.org/10.1515/jengeo-2016-0004.
[36] S. Ziaul, S. Pal, Analyzing control of respiratory particulate matter on Land Surface Temperature in local climate zones of English Bazar Municipality and Surroundings, Urban Climate 24 (2018) 34–50, https://doi.org/10.1016/j.uclim.2018.01.006.
[37] N. Schwarz, S. Lautenbach, R. Seppelt, Exploring indicators for quantifying surface urban heat islands of European cities with MODIS land surface temperatures, Remote Sens. Environ. 115 (2011) 3175–3186, https://doi.org/10.1016/j.rse.2011.07.003.
[38] Y.Y. Cui, B. de Foy, Seasonal variation of the urban heat island at the surface and the near-surface and reduction due to urban vegetation in Mexico city, J. Appl. Meteorol. Clim. 51 (2012) 855–868, https://doi.org/10.1175/JAMC-D-11-0104.1.
[39] M. Lazzarini, P.R. Marpu, H. Ghedira, Temperature-land cover interactions: the inversion of urban heat island phenomenon in desert city areas, Remote Sens. Environ. 130 (2013) 136–152, https://doi.org/10.1016/j.rse.2012.11.007.
[40] J. Wang, B. Huang, Future urban climatic map development based on spatio-temporal image fusion for monitoring the seasonal response of urban heat islands to land use/cover, The Urban Climatic Map: A Methodology for Sustainable Urban Planning, first ed., Routledge, New York, NY, USA, 2015.
[41] S. Haashemi, Q. Weng, A. Darvishi, S.K. Alavipanah, Seasonal variations of the surface urban heat island in a semi-arid city, Remote Sens-BASEL 8 (2016) 352, https://doi.org/10.3390/rs8040352.
[42] N. Benas, N. Chrysoulakis, C. Cartalis, Trend of urban surface temperature and heat island characteristics in the Mediterranean, Theor. Appl. Climatol. 130 (2017) 807–816, https://doi.org/10.1007/s00704-016-1913-8.

[43] V. Miles, I. Esau, Seasonal and spatial characteristics of urban heat islands (UHIs) in northern west siberian cities, Remote Sens-BASEL 9 (2017) 989, https://doi.org/10.3390/rs9100989.
[44] Y. Yuan, C. Xi, Q. Jing, N. Felix, Seasonal variations of the urban thermal environment effect in a tropical coastal city, Adv. Meteorol. (2017), https://doi.org/10.1155/2017/8917310 ID 8917310.
[45] M. Kottek, J. Grieser, C. Beck, B. Rudolf, F. Rubel, World Map of the Koppen-Geiger climate classification updated, Meteorol. Z. 15 (2006) 259–263, https://doi.org/10.1127/0941-2948/2006/0130.
[46] F. Leconte, J. Bouyer, R. Claverie, M. Pétrissans, Using Local Climate Zone scheme for UHI assessment: evaluation of the method using mobile measurements, Build. Environ. 83 (2015) 39–49, https://doi.org/10.1016/j.buildenv.2014.05.005.
[47] J. Geletič, M. Lehnert, GIS-based delineation of local climate zones: the case of medium-sized Central European cities, Morav. Geogr. Rep. 24 (2016) 2–12, https://doi.org/10.1515/mgr-2016-0012.
[48] Y. Zheng, C. Ren, Y. Xu, R. Wang, J. Ho, K. Lau, E. Ng, GIS-based mapping of Local Climate Zone in the high-density city of Hong Kong, Urban Climate 24 (2018) 419–448, https://doi.org/10.1016/j.uclim.2017.05.008.
[49] B. Bechtel, C. Daneke, Classification of local climate zones based on multiple earth observation data, IEEE J-STARS 5 (2012) 1191–1202, https://doi.org/10.1109/JSTARS.2012.2189873.
[50] E. Lélovićs, J. Unger, T. Gál, C.V. Gál, Design of an urban monitoring network based on Local Climate Zone mapping and temperature pattern modelling, Clim. Res. 60 (2014) 51–62, https://doi.org/10.3354/cr01220.
[51] T. Gál, B. Bechtel, J. Unger, Comparison of two different Local Climate Zone mapping methods, 9th International Conference on Urban Climate, Toulouse, 2015 http://real.mtak.hu/28577/1/GD2-6-1551002_a.pdf.
[52] U.S. Geological Survey (USGS), Department of the Interior, LANDSAT-8 (L8) Data Users Handbook (Version 2.0), (2016) https://landsat.usgs.gov/documents/Landsat8DataUsersHandbook.pdf , Accessed date: 20 September 2018.
[53] U.S. Geological Survey (USGS), Department of the Interior, LANDSAT-8 Surface Reflectance Code (LaSRC) Product (Version 4.3), (2018) https://landsat.usgs.gov/sites/default/files/documents/lasrc_product_guide.pdf , Accessed date: 20 September 2018.
[54] O. Rozenstein, Z. Qin, Y. Derimian, A. Karnieli, Derivation of land surface temperature for Landsat-8 TIRS using a split window algorithm, Sensors-BASEL 14 (2014) 5768–5780, https://doi.org/10.3390/s140405768.
[55] R.E. Livezey, Field intercomparison, in: H. von Storch, A. Navarra (Eds.), Analysis of Climate Variability: Applications of Statistical Techniques, second ed., Springer, New York, NY, USA; Heidelberg, Germany, 1995.
[56] R. Vázquez-Jiménez, R. Romero-Calcerrada, R.N. Ramos-Bernal, P. Arrogante-Funes, C.J. Novillo, Topographic correction to Landsat imagery through slope classification by applying the SCS + C method in mountainous forest areas, ISPRS Int. J. Geo-Inf. 6 (2017) 287, https://doi.org/10.3390/ijgi6090287.
[57] J. Rogan, M. Ziemer, D. Martin, S. Ratick, N. Cuba, V. DeLauer, The impact of tree cover loss on land surface temperature: a case study of central Massachusetts using Landsat Thematic Mapper thermal data, Appl. Geogr. 45 (2013) 49–57.
[58] E.S. Krayenhoff, J.A. Voogt, Daytime thermal anisotropy of urban neighbourhoods: morphological causation, Remote Sens-BASEL 8 (2016) 108, https://doi.org/10.3390/rs8020108.
[59] L. Hu, N.A. Brunsell, The impact of temporal aggregation of land surface temperature data for surface urban heat island (SUHI) monitoring, Remote Sens. Environ. 134 (2013) 162–174, https://doi.org/10.1016/j.rse.2013.02.022.
[60] P. Jönsson, Z. Cai, E. Melaas, M.A. Friedl, L. Eklundh, A method for robust estimation of vegetation seasonality from Landsat and sentinel-2 time series data, Remote Sens-BASEL 10 (2018) 635, https://doi.org/10.3390/rs10040635.
[61] J. Hu, P. Ghamisi, X. Zhu, Feature extraction and selection of sentinel-1 dual-pol data for global-scale local climate zone classification, ISPRS Int. J. Geo-Inf. 7 (2018) 379, https://doi.org/10.3390/ijgi7090379.
[62] Q. Chunping, M. Schmitt, M. Lichao, Z. Xiaoxiang, Urban Local Climate Zone Classification with a Residual Convolutional Neural Network and Multi-Seasonal Sentinel-2 Images, 10th IAPR Workshop on Pattern Recognition in Remote Sensing, PRRS, 2018, pp. 1–5.
[63] P. Dobrovolný, The surface urban heat island in the city of Brno (Czech Republic) derived from land surface temperatures and selected reasons for its spatial variability, Theor. Appl. Climatol. 112 (2013) 89–98, https://doi.org/10.1007/s00704-012-0717-8.
[64] M. Cai, C. Ren, Y. Xu, K.K.L. Lau, R. Wang, Investigating the relationship between local climate zone and land surface temperature using an improved WUDAPT methodology - a case study of Yangtze River Delta, China, Urban Climate 24 (2018) 485–502, https://doi.org/10.1016/j.uclim.2017.05.010.
[65] L. Sheng, X. Tang, H. You, Q. Gu, H. Hu, Comparison of the urban heat island intensity quantified by using air temperature and Landsat land surface temperature in Hangzhou, China, Ecol. Indicat. 72 (2017) 738–746, https://doi.org/10.1016/j.ecolind.2016.09.009.
[66] W. Liu, J. Feddema, L. Hu, A. Zung, N. Brunsell, Seasonal and diurnal characteristics of land surface temperature and major explanatory factors in Harris County, Texas, Sustainability-BASEL 9 (2017) 2324, https://doi.org/10.3390/su9122324.
[67] B. Yang, F. Meng, X. Ke, C. Ma, The impact analysis of water body landscape pattern on urban heat island: a case study of Wuhan city, Adv. Meteorol. (2015), https://doi.org/10.1155/2015/416728 ID 416728.
[68] C.R. Wood, L. Pauscher, H.C. Ward, S. Kotthaus, J.F. Barlow, M. Gouvea, S.E. Lane, C.S.B. Grimmond, Wind observations above an urban river using a new lidar technique, scintillometry and anemometry, Sci. Total Environ. 442 (2013) 527–533, https://doi.org/10.1016/j.scitotenv.2012.10.061.
[69] J. Desplat, R. Kounkou-Arnaud, EPICEA, la meteorologie urbaine au service de al Ville de Paris, Meteorol. Mag. 9 (2010) 13–15.
[70] F. Mancebo, Gardening the city: addressing sustainability and adapting to global warming through urban agriculture, Environments 5 (2018) 38, https://doi.org/10.3390/environments5030038.
[71] K. Ward, S. Lauf, B. Kleinschmit, W. Endlicher, Heat waves and urban heat islands in Europe: a review of relevant drivers, Sci. Total Environ. 569 (2016) 527–539, https://doi.org/10.1016/j.scitotenv.2016.06.119.
[72] M.L. Imhoff, P. Zhang, R.E. Wolfe, L. Bounoua, Remote sensing of the urban heat island effect across biomes in the continental USA, Remote Sens. Environ. 114 (2010) 504–513, https://doi.org/10.1016/j.rse.2009.10.008.
[73] H. Akbari, D.M. Kurn, S.E. Bretz, J.W. Hanford, Peak power and cooling energy savings of shade trees, Energy Build. 25 (1997) 139–148.
[74] Á. Gulyás, J. Unger, A. Matzarakis, Assessment of the microclimatic and human comfort conditions in a complex urban environment: modelling and measurements, Build. Environ. 41 (2006) 1713–1722, https://doi.org/10.1016/j.buildenv.2005.07.001.
[75] S. Gillner, J. Vogt, A. Tharang, S. Dettmann, A. Roloff, Role of street trees in mitigating effects of heat and drought at highly sealed urban sites, Landsc. Urban Plann. 143 (2015) 33–42, https://doi.org/10.1016/j.landurbplan.2015.06.005.
[76] W. Klemm, B.G. Heusinkveld, S. Lenzholzer, B. van Hove, Street greenery and its physical and psychological impact on thermal comfort, Landsc. Urban Plann. 138 (2015) 87–98, https://doi.org/10.1016/j.landurbplan.2015.02.009.
[77] J. Mullaney, T. Lucke, S.J. Trueman, A review of benefits and challenges in growing street trees in paved urban environments, Landsc. Urban Plann. 134 (2015) 157–166, https://doi.org/10.1016/j.landurbplan.2014.10.013.
[78] M.A. Hart, D.J. Sailor, Quantifying the influence of land-use and surface characteristics on spatial variability in the urban heat island, Theor. Appl. Climatol. 95 (2009) 397–406, https://doi.org/10.1007/s00704-008-0017-5.
[79] D.E. Bowler, L. Buyung-Ali, T.M. Knight, A.S. Pullin, Urban greening to cool towns and cities: a systematic review of the empirical evidence, Landsc. Urban Plann. 97 (2010) 147–155, https://doi.org/10.1016/j.landurbplan.2010.05.006.
[80] P.A. Dugord, S. Lauf, C. Schuster, B. Kleinschmit, Land use patterns, temperature distribution, and potential heat stress risk - the case study Berlin, Germany, Comput. Environ. Urban Syst. 48 (2014) 86–98, https://doi.org/10.1016/j.compenvurbsys.2014.07.005.
[81] M. Maimaitiyiming, A. Ghulam, T. Tiyip, F. Pla, P. Latorre-Carmona, U. Halik, M. Caetano, Effects of green space spatial pattern on land surface temperature: implications for sustainable urban planning and climate change adaptation, ISPRS J. Photogramm. 89 (2014) 59–66, https://doi.org/10.1016/j.isprsjprs.2013.12.010.